

12-2013

# Co-Design of Multi-Band High-Efficiency Power Amplifier and Three-Pole High-Q Tunable Filter

Kenle Chen

*Purdue University*, chen314@purdue.edu

Tsung-Chieh Lee

*Purdue University*, lee640@purdue.edu

Dimitrios Peroulis

*Purdue University, Birck Nanotechnology Center*, dperouli@purdue.edu

Follow this and additional works at: <http://docs.lib.purdue.edu/nanopub>



Part of the [Nanoscience and Nanotechnology Commons](#)

---

Chen, Kenle; Lee, Tsung-Chieh; and Peroulis, Dimitrios, "Co-Design of Multi-Band High-Efficiency Power Amplifier and Three-Pole High-Q Tunable Filter" (2013). *Birck and NCN Publications*. Paper 1548.

<http://docs.lib.purdue.edu/nanopub/1548>

This document has been made available through Purdue e-Pubs, a service of the Purdue University Libraries. Please contact [epubs@purdue.edu](mailto:epubs@purdue.edu) for additional information.

# Co-Design of Multi-Band High-Efficiency Power Amplifier and Three-Pole High- $Q$ Tunable Filter

Kenle Chen, *Student Member, IEEE*, Tsung-Chieh Lee, *Student Member, IEEE*, and Dimitrios Peroulis, *Member, IEEE*

**Abstract**—This letter reports a novel methodology for co-design of broadband power amplifiers (PAs) and high- $Q$  tunable filters. It is for the first time demonstrated that the tunable filter's input port can be synthesized to directly match the transistor's output, thus eliminating the conventional broadband/band-reconfigurable matching network of the PA. This leads to minimized circuit size, volume, and loss. In this letter, a three-pole tunable bandpass filter is designed as the output matching network of a 10 W GaN PA, yielding optimal fundamental and harmonic impedances. Simulation and measured results show that the co-designed PA-filter module exhibits desired Chebyshev filter behavior while achieving efficient PA performance in the passband over a 400-MHz tuning range from 2.95–3.35 GHz. Specifically, 51%–67% efficiency,  $\approx 10$  W output power,  $\approx 10$  dB gain were measured throughout the entire frequency range.

**Index Terms**—Co-design, efficiency, filter, multi-band, power amplifier (PA), quality factor, tunable.

## I. INTRODUCTION

IN modern wireless transmitters, high power amplifiers are typically followed by post-select bandpass filters (BPFs) to ensure required spectral characteristics for transmission. Future intelligent RF front-ends, e.g., software-defined radio, are required to support multi-band/standard operations. Therefore, wideband PAs and tunable filters are key enabling technologies for such systems. Recently, there have been significant advances in design and realization of both broadband PAs [1]–[3] and widely-tunable filters [4], achieving record high multi-band performances comparable to traditional single-band designs.

It is important to note that these designs are mostly based on the classical microwave/RF philosophy that the PAs and filters are designed independently assuming 50- $\Omega$  matching conditions. However, given the non-negligible insertion loss of a tunable filter, inter-connection mismatch, and the lossy tunable matching network of PA, the overall performance of a PA-filter module may be considerably degraded. To avoid such difficulties, it is attractive to consider co-designing PAs and filters. Particularly, the PA output matching network can be entirely eliminated by designing the filter input impedance to directly match

Manuscript received May 20, 2013; revised August 16, 2013; accepted August 22, 2013. Date of publication October 08, 2013; date of current version November 28, 2013. This work was supported by the Defense Advanced Research Projects Agency (DARPA) under the Seedling Evanescent-Mode Cavity program.

The authors are with the School of Electrical and Computer Engineering and Birck Nano Technology Center, Purdue University, West Lafayette, IN, 47906 USA (e-mail: chen314@purdue.edu; dperouli@purdue.edu).

Color versions of one or more of the figures in this paper are available online at <http://ieeexplore.ieee.org>.

Digital Object Identifier 10.1109/LMWC.2013.2283876

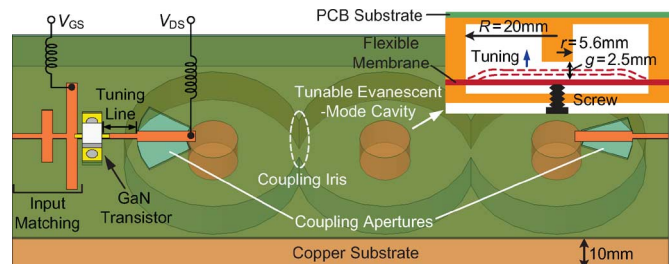


Fig. 1. 3-D illustration of PA with a tunable three-pole evanescent-mode filter.

the transistor, leading to smaller size/volume, reduced loss, and enhanced overall performance.

This co-design concept has been proposed and investigated for PAs with single resonators [5], [6] and a static two-pole filter [7]. In this research, we present, for the first time, the integration of PA and three-pole tunable filter, achieving  $> 30$  dB improvement of isolation at  $\Delta f = 10\%f_0$  compared our prior works. Further, the filter is first demonstrated using entirely metallic cavities, which are more realistic than the substrate-integrated cavities in [5]–[7]. The implemented PA-filter module exhibits the desired filter response with efficient PA performance in the passband, while being continuously tunable over a 350-MHz band.

## II. MATCHING FILTER THEORY

Fig. 1 shows the three-dimensional (3-D) illustration of the co-designed PA and filter. It can be seen that the microwave cavity filter is directly connected to the transistor's drain node, and no matching network is employed. The key enabler for this co-design technique is the matching filter, which not only needs to provide desired frequency selectivity, but is also required to act as a matching network for the transistor.

In this investigation, a third-order Chebyshev-response BPF is designed with 20 dB equi-ripple return loss. Such a filter can be represented by a  $(N + 2) \times (N + 2)$  normalized coupling matrix, given by

$$\mathbf{M} = \begin{bmatrix} 0 & M_{S1} & 0 & 0 & 0 \\ M_{S1} & M_{11} & M_{12} & 0 & 0 \\ 0 & M_{12} & M_{22} & M_{23} & 0 \\ 0 & 0 & M_{23} & M_{33} & M_{4L} \\ 0 & 0 & 0 & M_{4L} & 0 \end{bmatrix} \quad (1)$$

where  $M_{S1}$  and  $M_{4L}$  denote input and output external couplings, respectively, while  $M_{12}$  and  $M_{23}$  represent inter-resonator couplings.  $M_{11}$ ,  $M_{22}$  and  $M_{33}$  stand for the detuning of each resonator's resonant frequency from the center frequency of the filter's frequency response. For the filter with the coupling

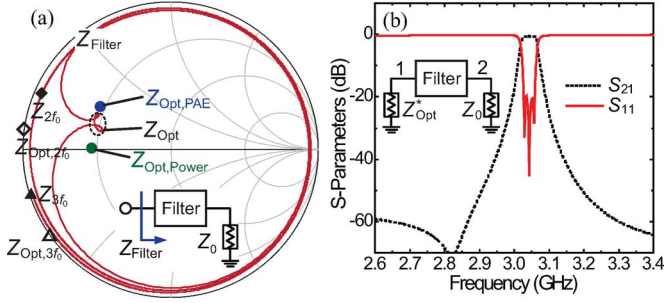


Fig. 2. Matching filter design: (a) load-pull results and input impedance trajectory, (b) frequency response of the designed filter.

matrix (1), the normalized impedance seen into its input port at  $f_0$  is given by [8]

$$Z_{in} = \frac{M_{4L}^2 + jM_{11}}{M_{S1}^2} \quad (2)$$

assuming  $M_{22}$  and  $M_{33}$  are both zero. The derived coupling matrix for a regular third-order Chebyshev BPF with 20 dB equi-ripple return loss is

$$\mathbf{M} = \begin{bmatrix} 0 & 1.0825 & 0 & 0 & 0 \\ 1.0825 & 0 & 1.0302 & 0 & 0 \\ 0 & 1.0302 & 0 & 1.0302 & 0 \\ 0 & 0 & 1.0302 & 0 & 1.0825 \\ 0 & 0 & 0 & 1.0825 & 0 \end{bmatrix}. \quad (3)$$

As indicated in (2),  $Z_{in}$  can be set to any wanted values by modifying  $M_{S1}$  and  $M_{11}$ , while maintaining the same Chebyshev filter response as the regular case [8].

The filter is physically built using evanescent-mode cavity resonators [4], as shown in Fig. 1. This type of resonator is constructed by placing a loading post at the center of a cylindrical cavity. The resonant frequency can be shifted by changing the gap spacing between the bottom wall and the center post, which is realized in this work using a tuning screw as depicted in the inset of Fig. 1. In this third-order filter design, three EVA resonators are coupled through coupling irises, forming the mutual coupling coefficients ( $M_{12}$  and  $M_{23}$ ). The external couplings ( $M_{S1}$  and  $M_{4L}$ ) are realized using the slot apertures, whose size determines the coupling strength.

### III. CO-DESIGN AND IMPLEMENTATION OF PA-FILTER

A 10 W GaN transistor (Cree CGH40010F) is utilized in this design. Its desired output impedance at 3 GHz is extracted from load-pull simulations, as indicated in Fig. 2(a). It is found in the simulation that the regular efficiency-optimized or power-optimized impedance is not the optimal point for the co-design of PA and filter in terms of filter shape and PA efficiency performance. In this design, the filter input impedance is set to a point ( $Z_{Opt.} \approx 13 + 5j\Omega$ ) in between  $Z_{Opt.,PAE}$  and  $Z_{Opt.,Power}$  as shown in Fig. 2(a). This yields desired filter frequency response while maintaining  $>70\%$  efficiency within the filter passband, shown in Fig. 3.

The real part of  $13\Omega$  is created by increasing the input coupling ( $M_{S1}$ ) from 1.0825 to 2.0925, which is physically realized by enlarging the input coupling aperture as indicated in Fig. 1. The small imaginary part of  $5\Omega$  is achieved by placing a tuning line between the transistor and the intrinsic filter, as

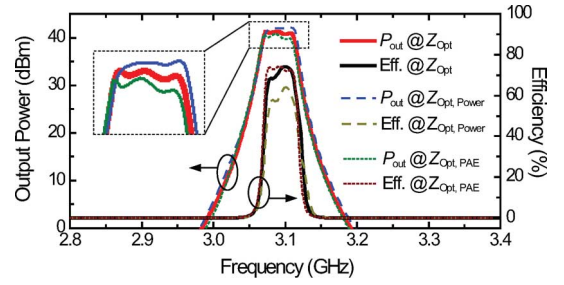


Fig. 3. Simulated large-signal frequency response of the co-designed PA-filter under 30 dBm input stimulus.

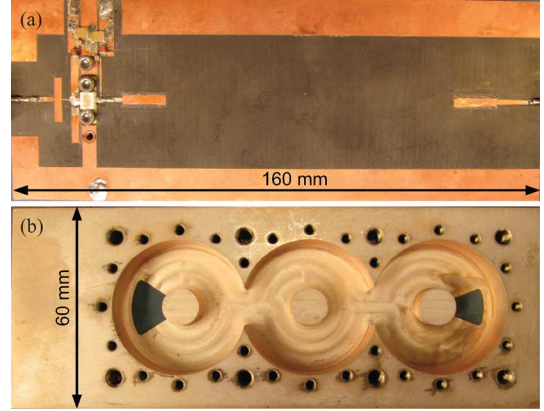


Fig. 4. Fabricated PA-filter co-design module: (a) front side, (b) back side.

indicated in Fig. 1. We can have a non-zero  $M_{11}$  to perfect the imaginary part when the filter is tuned to other frequencies. Fig. 2(a) show the input impedance of the designed filter, ( $Z_{Filter}$ , varying from 2.6–9.3 GHz). It presents an expected Chebyshev filter shape with 1.7% bandwidth, 0.56 dB insertion loss, and 20 dB equi-ripple return loss, as indicated in Fig. 2(b). The unloaded quality factor of the EVA resonator is around 2500, extracted from full Wave simulation.

The input matching network is designed using a two-stage lowpass network implemented with transmission lines [1], as shown in Fig. 1. Fig. 4 illustrates the fabricated circuit of the co-designed PA and filter module. The PA circuit is printed on a Rogers 5880 PCB board [Fig. 4(a)], which is laminated on the copper substrate containing evanescent-mode cavities [Fig. 4(b)]. The gate bias is applied through a  $250\Omega$  resistor and a 17 nH inductor. A high-impedance short-circuited stub is appended to the tuning line to supply the drain bias. This bias line is also utilized to further optimize the harmonic impedances presented to the transistor, which are very closed to the optimal points as indicated in Fig. 2(a).

### IV. EXPERIMENTAL RESULTS

Small-signal measurement is first conducted with the fabricated PA-filter module to determine its frequency response and tuning range. Fig. 5(a) shows the measured S-parameters when the circuit is operating at 3.08 GHz. A perfect Chebyshev filter shape is achieved with 15.5 dB small-signal gain in the passband and 3 dB bandwidth of 54 MHz ( $\approx 1.7\%$ ). Simulation results are also shown in Fig. 5(a) indicating a good agreement with the measurements. The achieved equi-ripple return loss is increased to 10 dB, compared to the static case in Fig. 2(b), mainly due to the load-line matching condition applied in the PA design.

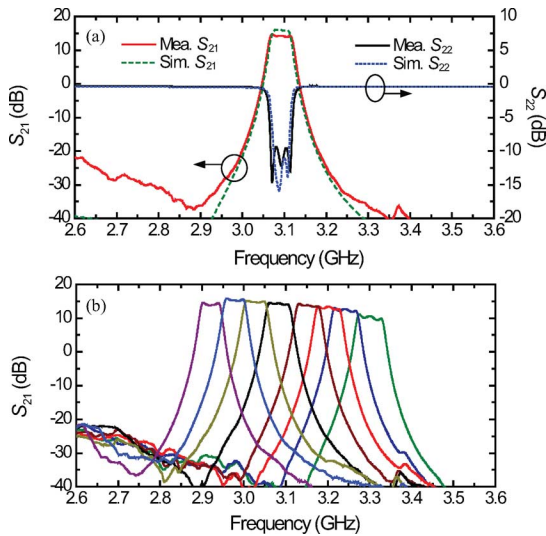


Fig. 5. Small-signal frequency response: (a) measured and simulated results at 3.1 GHz, (b) measurement over the entire tuning range.

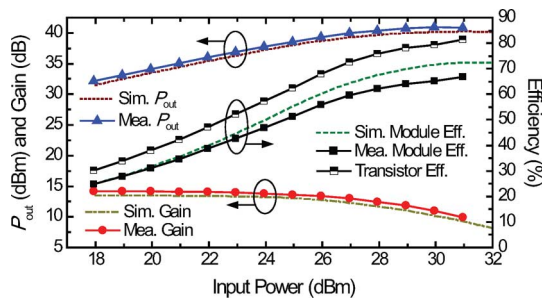


Fig. 6. Measured PA performance versus input power at 3.1 GHz.

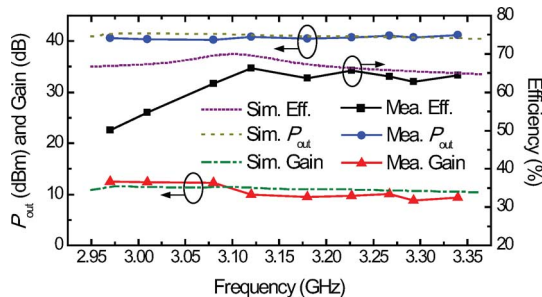


Fig. 7. Measured PA performance over the entire tuning range.

TABLE I  
COMPARISON WITH STATE-OF-THE-ART CONVENTIONAL PAs

Refs.	OMN	$f$ (GHz)	$P$ (W)	Max. Eff.	Band Selectivity
2011 [1]	TLs/LPF*	0.9–2.2	15	86%	None
2011 [2]	TLs/LPF	1.3–2.7	11	70%	None
2012 [3]	TLs/LPF	1.45–2.45	14.5	81%	None
This work	Cavity/BPF	2.95–3.35	10	67%/82%	High

\* LPF denotes Lowpass filter.

Fig. 5(b) shows the tunable range of this PA-filter module. Desired filter response and pass-band performance ( $> 10$  dB gain) are achieved when the circuit is tuning from 2.95–3.35 GHz. The gain drops at higher frequencies due to the change of input impedance, since the physically realized coupling coefficients are very sensitive to frequency. A possible way to compensate this is to incorporate additional degrees of tunability in coupling structures [4].

Then, the large-signal measurements are carried out. Fig. 6 shows the measured PA performance under various input powers when the circuit operating at the center frequency of 3.1 GHz. The PA gain starts to compress at a input power of 24 dBm. The highest PA efficiency of 67% is achieved at a gain compression of  $\approx 2$  dB with a maximum output power of 40 dBm. Simulation results are also plotted in Fig. 6 for comparison. The measured PA performance is slightly lower than the simulated one, mainly caused by the degraded quality factor of the resonators due to the fabrication inaccuracies and imperfections. The measured efficiency can be de-embedded to the transistor by subtracting the simulated filter loss from the original data. Thus, the equivalent transistor efficiency is around 82% as shown in Fig. 6, which is consistent with the state-of-the-art PAs as listed in Table I. Fig. 7 shows the measured PA performance at the maximum power level over the entire tuning range. Around 40 dBm output power, 10 dB gain, and 51%–67% efficiency were measured. It is noted that the efficiency drops below in the lower frequency range below 3.05 GHz. This is due to the fact that when tuning the frequency down, the screw needs to largely push down the flexible membrane, leading to a protuberance in the internal surface of the cavity which degrades the cavity's  $Q_u$ .

## V. CONCLUSION

The co-design of a broadband PA and high- $Q$  tunable filter is presented in this letter. By synthesizing the filter's input to directly match the transistor's output, the conventional output matching network of the PA is entirely eliminated, minimizing the circuit size, volume, and loss. In this letter, a three-pole tunable BPF is co-designed with a 10 W GaN PA as its OMN, yielding optimal fundamental and harmonic impedances. The implemented co-designed PA-filter module exhibits desired filter response and efficient PA performance when tuning from 2.95–3.35 GHz. Specifically, 51%–67% efficiency,  $\approx 10$  W output power,  $\approx 10$  dB gain were measured throughout the entire tuning range.

## REFERENCES

- [1] K. Chen and D. Peroulis, "Design of highly efficient broadband class-E power amplifier using synthesized lowpass matching networks," *IEEE Trans. Microw. Theory Tech.*, vol. 59, no. 12, pp. 3162–3173, Dec. 2011.
- [2] J. Kim, J. Kim, J. Moon, J. Son, I. Kim, J. Jee, and B. Kim, "Saturated power amplifier optimized for efficiency using self-generated harmonic current and voltage," *IEEE Trans. Microw. Theory Tech.*, vol. 59, no. 8, pp. 2049–2058, Aug. 2011.
- [3] N. Tuffy, L. Guan, A. Zhu, and T. J. Brazil, "A simplified broadband design methodology for linearized high-efficiency continuous class-F power amplifiers," *IEEE Trans. Microw. Theory Tech.*, vol. 60, no. 6, pp. 1952–1963, Jun. 2012.
- [4] H. Joshi, H. H. Sigmarsson, S. Moon, D. Peroulis, and W. J. Chappell, "High- $Q$  fully reconfigurable tunable bandpass filter," *IEEE Trans. Microw. Theory Tech.*, vol. 57, no. 12, pp. 3525–3533, Dec. 2009.
- [5] K. Chen, X. Liu, W. J. Chappell, and D. Peroulis, "Co-design of power amplifier and narrowband filter using high- $Q$  evanescent-mode cavity resonator as the output matching network," in *IEEE MTT-S Int. Dig.*, Jun. 2011, pp. 1–4.
- [6] K. Chen, X. Liu, and D. Peroulis, "Widely-tunable high-efficiency power amplifier with ultra-narrow instantaneous bandwidth," *IEEE Trans. Microw. Theory Tech.*, vol. 60, no. 12, pp. 3787–3797, Dec. 2012.
- [7] K. Chen, J. Lee, W. J. Chappell, and D. Peroulis, "Co-design of highly efficient power amplifier and high- $Q$  output bandpass filter," *IEEE Trans. Microw. Theory Tech.*, to be published.
- [8] M. Meng and K.-L. Wu, "Direct synthesis of general Chebyshev bandpass filters with a frequency variant complex load," in *IEEE MTT-S Int. Dig.*, May 2010, pp. 433–436.